

# Characteristics of laser and current pulses in a He–SrCl<sub>2</sub> vapor laser

L. Chen · B.-L. Pan · Y.-J. Wang · Q. Zhu · X.-Y. Zhang

Received: 18 June 2009 / Revised version: 12 September 2009 / Published online: 13 October 2009  
© Springer-Verlag 2009

**Abstract** An experimental investigation on the characteristics of laser and current pulses in a He–SrCl<sub>2</sub> vapor laser is carried out. The temporal dependences of the discharge current pulse on the laser pulses at the 1.09 μm, ~3 μm and 6.45 μm lines in strontium atoms and ions are measured and analyzed under different laser output powers. It is found that all laser pulses appear at the falling edge of the current pulse and shift forward to the current pulse with increasing laser output power.

**PACS** 42.55.Lt · 42.60.Jf

## 1 Introduction

A lot of research on the output performance and the lasing mechanism of the strontium vapor laser excited by the high repetition rate pulsed discharge has been done during the past decades [1–4], since Deech et al. first observed the mid-infrared laser transitions in strontium vapor [5]. It was found that the strontium vapor laser has the characteristics of multiple laser lines operating in the 416.2 nm–6.45 μm spectral range with higher lasing efficiency and output power of several watts, which may find many applications in material processing, micro-electronic technology, laser medical treatment, infrared technology and so on [6–10]. Thus, scientists all over the world make a great effort to improve the output characteristics of the strontium ionic and atomic lasers. Platonov et al. once reported a strontium vapor laser operating at 6.45 μm laser line with a relative high output power

of 1.2 W [11]. By increasing the active volume and optimizing the working parameters, a sealed-off strontium vapor laser with 2.5 W output power was reported in [12]. To solve the problem of the intense chemical reaction between the strontium vapor and the surface of the discharge tube in a pure strontium vapor laser, the SrBr<sub>2</sub> material was successfully used to replace the metallic strontium as the lasant, and multi-line laser oscillations were realized [13]. Recently, the maximum multi-line output power of 4.26 W was obtained in He–SrBr<sub>2</sub> pulsed discharge with large active volume and IC excitation circuit [14]. A mathematical model for the alternate oscillations of the 430 nm Sr<sup>+</sup> recombination laser and the 1.09 μm RM transition laser was established to understand their kinetic process and lasing mechanism [15], and the relationship between the simulated current and laser pulses were found to be in good agreement with that in experiment. The output characteristic of a He–SrCl<sub>2</sub> laser was reported with the power specific of 12.5 mW/cm<sup>3</sup> [16], which is comparable to that obtained in [10].

Since the lasing process of the He–SrCl<sub>2</sub> vapor laser is different from the pure strontium vapor laser due to the dissociation and recombination of SrCl<sub>2</sub> molecules in the pulsed discharge period, it is important to do an investigation of the photo-electrical pulse characteristic of the He–SrCl<sub>2</sub> vapor laser for understanding its lasing process and improving its output performance. In this paper, the discharge current and the laser pulses at 1.09 μm, ~3 μm and 6.45 μm lines of the pulsed He–SrCl<sub>2</sub> vapor laser are detected simultaneously and compared under different output powers of 144 mW~864 mW by varying the voltage from HV rectifier, the pulsed repetition frequency in the range of 4.8 kV~5.6 kV, 15.7 kHz~17 kHz, respectively with the constant helium pressure of 40 torr. The dependence of the laser pulse at each line on the output power and the temporal relations between all laser pulses and the current pulse are

L. Chen · B.-L. Pan (✉) · Y.-J. Wang · Q. Zhu · X.-Y. Zhang  
Department of Physics, Zhejiang University, 310027 Hangzhou,  
China  
e-mail: pbl66@zju.edu.cn

measured and analyzed. It is shown that all laser pulses start at the falling edge of the current pulse and shift forward to the current pulse with the increase of the laser power, which is totally different from those observed in the pure strontium vapor laser [12, 17]. Some reasons are given to explain this phenomenon.

## 2 Experimental setup

The experimental setup is presented in Fig. 1. The laser tube is composed of a basic quartz tube of 36 mm inner diameter and a ceramic tube of 15 mm inner diameter and 60 cm length to confine the active volume. A thin layer of alumina fiber between the ceramic tube and the quartz one is used to avoid damaging the quartz tube from the high temperature and the interlayer discharge channel. The quartz tube is wrapped by another layer of alumina fiber for thermal insulation. The temperature on the surface of alumina fiber is measured by a thermal meter and keeps a relative optimal value of 423 K by changing the input power and the thickness of the alumina fiber as described in [16]. The  $\text{SrCl}_2$  powder of 99% purity is uniformly put on the ceramic tube and the required  $\text{SrCl}_2$  vapor density for lasing is obtained by discharge heating. Two pieces of  $\text{CaF}_2$  parallel plates are used as windows so as not to absorb the laser lines at  $\sim 3 \mu\text{m}$  and  $6.45 \mu\text{m}$ . The optical cavity in the length of 180 cm consists of a gold-coated reflection mirror and a  $\text{CaF}_2$  flat output mirror, and the electrode's separation is 65 cm.

The modified Blumein circuit is employed to excite the  $\text{SrCl}_2$  vapor laser, whose capacitance matches ( $C_1:C_2$ ) are optimized experimentally. The switch  $T$  is a hydrogen thyratron ZQM-2000/35. Helium of 99.99% purity is used as the buffer gas. The output power is measured by a THORLABS model PM100 power meter. The spectral selection is made through a set of glass and quartz plates having the high transmission in the different spectral range and the high absorption at  $6.45 \mu\text{m}$  [18]. The discharge voltage and the current

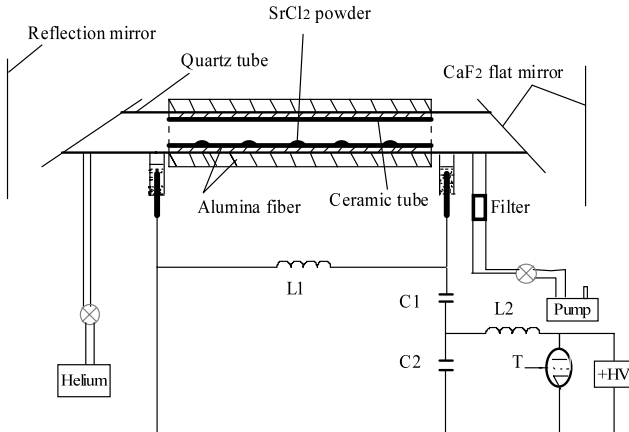


**Fig. 1** Experimental setup of the He– $\text{SrCl}_2$  vapor laser

pulses are detected by a Tektronix P6015 high voltage probe and a Pearson model 410 current transformer. THERLABS DET100 and VIGO pvm-10.6 infrared detectors are used to measure the laser pulses at  $1.09 \mu\text{m}$ ,  $\sim 3 \mu\text{m}$  lines and

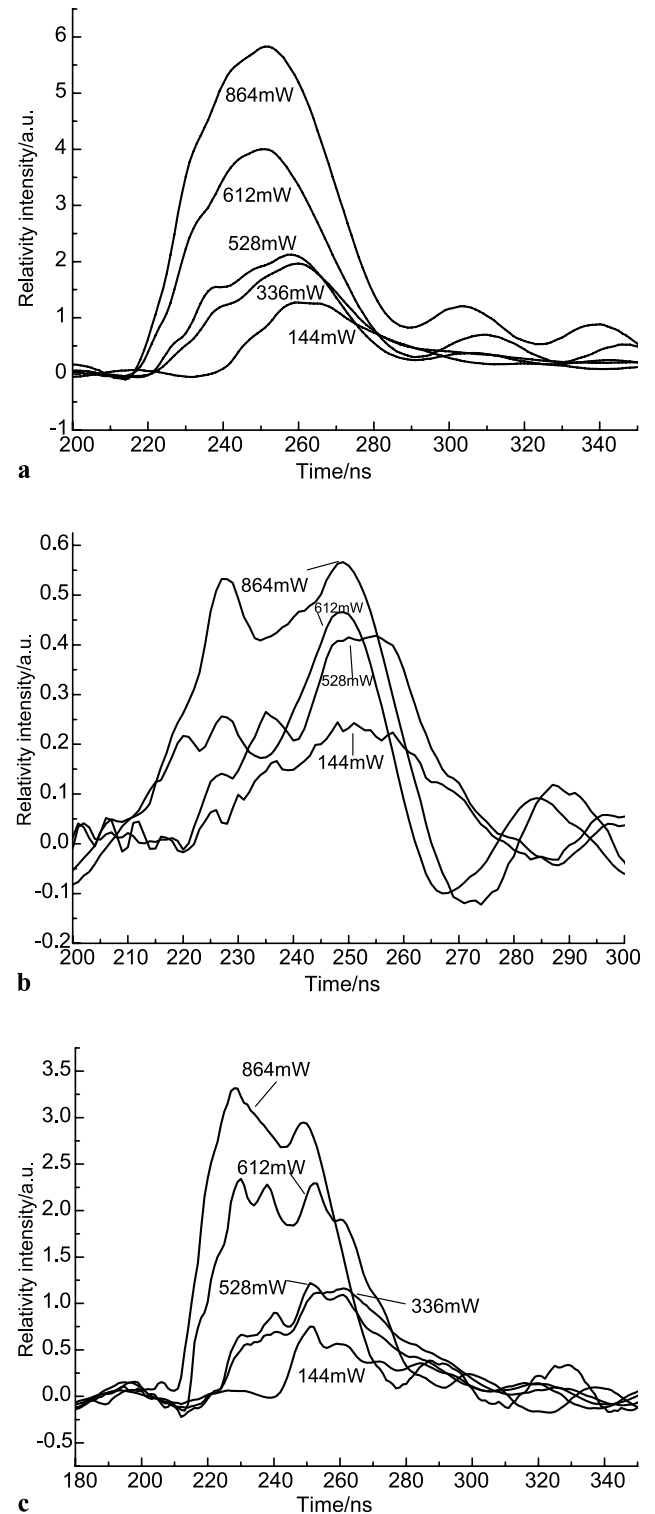


**Fig. 2** Dependences of laser pulses on the output power at  $1.09 \mu\text{m}$  (a),  $\sim 3 \mu\text{m}$  (b) and  $6.45 \mu\text{m}$  (c) lines

6.45 μm lines, respectively. All pulses are displayed on a Tektronix TDS 754C oscilloscope.

### 3 Experimental results and discussion

The laser and current pulses with different laser output powers are measured by changing the working parameters in the range mentioned above. After the stable operation of the He-SrCl<sub>2</sub> vapor laser, the three including the current pulse and the laser pulse with the electromagnetic noise and the only noise signal made by the high repetition rate pulsed discharge are recorded as data files, which can be processed to plot the real current and laser pulses by the original software.

Dependences of laser pulses on the output power are shown in Fig. 2 at 1.09 μm (a), ~3 μm (b) and 6.45 μm (c) lines. From Fig. 2, it can be seen that all the laser pulses are shifted forwards a little on the time axis and their relative intensity enhances gradually with the increase of the output power. The delay time between the maximum and the minimum laser pulse is up to about 10 ns. The pulse durations at 1.09 μm and ~3 μm lines are almost constant at the value of 64 ns and 58 ns respectively, while that at the 6.45 μm line changes in the range of 60 ns ~80 ns with the output power.

To explain the phenomena of the laser pulse shift mentioned above, the dependences of the laser output power and the electric power specific on the practical electric input power calculated by the measured current and voltage pulses in experiment are plotted in Fig. 3. One can see that the laser output power and the electric power specific have approximately a linear positive correlation with the practical electric input power. It is well known that the SrCl<sub>2</sub> vapor density and the electron temperature increase with increasing the electric input power, which is helpful to excite the

upper laser level, and it forms the population inversion in advance, finally resulting in the earlier occurrence of the laser pulse under the higher input power condition. Meanwhile the higher electron temperature on the higher input power condition is worse for de-excitation of the lower level of

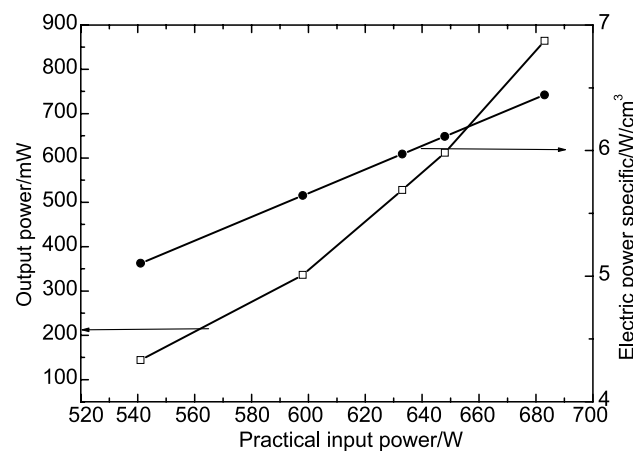
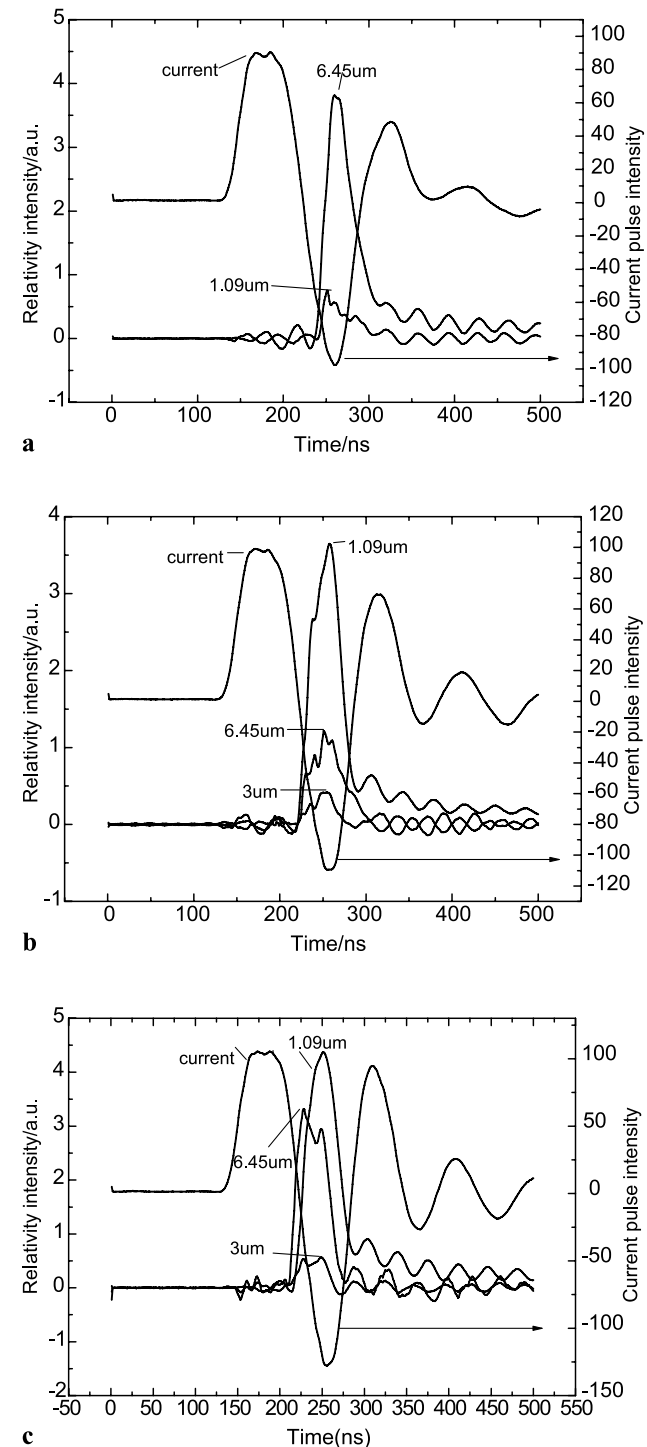


**Fig. 3** Dependence of the laser output power and the electric power specific on the practical input power in the tube

**Fig. 4** Temporal behaviors of the laser and current pulse under the various output power at the value of 144 mW (a), 528 mW (b), 864 mW (c)

these lasers, which causes the termination of the laser pulse more quickly.

Temporal behaviors of the laser and current pulse under the various laser output powers are shown in Fig. 4(a), (b) and (c). It can be found that the duration of the positive and negative current pulses are about 94 ns and their amplitudes are near the same. All of the laser pulses appear at the falling edge of the current pulse and are shifted forwards to the current pulse with increasing the laser output power, which greatly differs from those observed in the pure strontium vapor laser. The simulation result in [17] demonstrates that the laser pulse at 1.09  $\mu\text{m}$  appears at the rising edge of the current pulse, while the laser pulses at  $\sim 3 \mu\text{m}$  appear at the falling edge of the current pulse and the laser pulse at 6.45  $\mu\text{m}$  line follows the evolution of the current pulse. This can partially be explained by the decomposition and the recombination of SrCl<sub>2</sub> molecules during the pulsed discharge period and the different lasing processes considered in [17]. For reaching the threshold strontium vapor density, the SrCl<sub>2</sub> molecules need enough time and energy to be decompounded during the first positive current pulse, for which the whole laser pulse is delayed, and still existing in the negative current pulse. In Fig. 4(a) the laser pulse at  $\sim 3 \mu\text{m}$  is not produced because of the little gain of this kind of laser. The intensity of laser pulses between 1.09  $\mu\text{m}$  and  $\sim 3 \mu\text{m}$ , 6.45  $\mu\text{m}$  could not be compared due to the different attenuation of the two detectors to be measured.

#### 4 Conclusion

The characteristics of laser and current pulses in a He–SrCl<sub>2</sub> vapor laser are investigated and analyzed. It is found that all laser pulses at 1.09  $\mu\text{m}$ ,  $\sim 3 \mu\text{m}$  and 6.45  $\mu\text{m}$  lines appear at the falling edge of the current pulse and shift forward to the current pulse with increasing laser output power. Some possible reasons to explain the different temporal behavior of the current and laser pulses between the pure strontium

and SrCl<sub>2</sub> vapor lasers are presented. Our experimental results and analysis provide some scientific suggestion for understanding the lasing mechanism and improving the output performance of the pulsed discharge-excited He–SrCl<sub>2</sub> vapor laser.

**Acknowledgements** This research was supported by the National Natural Science Foundation of China under Grant No. 10974176 and Zhejiang Natural Science Foundation under Grant No. Y1090087.

#### References

1. M.F. Sem, I.G. Ivanov, Proc. SPIE **3403**, 120 (1998)
2. B.L. Pan, G. Chen, X. Chen, Z.X. Yao, J. Appl. Phys. **96**, 34 (2004)
3. M.S. Butler, J.A. Piper, Appl. Phys. Lett. **43**, 823 (1983)
4. B.L. Pan, G. Chen, J.W. Zhong, Z.X. Yao, Appl. Phys. B **76**, 371 (2003)
5. J.S. Deech, J.H. Sanders, IEEE J. Quantum Electron. **4**(7), 474 (1968)
6. Y. Takeda, A. Iwata, S. Ueguri, K. Fujii, IEEE J. Quantum Electron. **30**, 1176 (1994)
7. Y.J. Wang, B.L. Pan, L. Chen, B.N. Mao, Opt. Commun. **281**, 5405 (2008)
8. K.A. Temelkov, N.K. Vuchkov, B.L. Pan, N.V. Sabotinov, B. Ivanov, L. Lyutov, J. Phys. D, Appl. Phys. **39**, 3769 (2006)
9. Y.B. Wang, B.N. Mao, L. Chen, L.M. Wang, B.L. Pan, Acta Phys. Sin. **57**, 219 (2008)
10. K.A. Temelkov, N.K. Vuchkov, I. Freijo-Martin, A. Lema, L. Lyutov, N.V. Sabotinov, J. Phys. D, Appl. Phys. **42**, 115105 (2009)
11. V. Platonov, A.N. Soldatov, A.G. Filonov, Sov. J. Quantum Electron. **8**(1), 120 (1978)
12. A.N. Soldatov, A.G. Filonov, A.S. Shumeiko, A.E. Kirilov, Proc. SPIE **5483**, 252 (2004)
13. B.L. Pan, Z.X. Yao, G. Chen, Chin. Phys. Lett. **19**, 941 (2002)
14. K.A. Temelkov, N.K. Vuchkov, B.N. Mao, E.P. Atanassov, L. Lyutov, N.V. Sabotinov, IEEE J. Quantum Electron. **45**, 278 (2009)
15. L. Chen, B.N. Mao, Y.B. Wang, L.M. Wang, B.L. Pan, Opt. Commun. **281**, 1211 (2008)
16. L. Chen, B.L. Pan, Y.J. Wang, K.A. Temelkov, N.K. Vuchkov, Opt. Commun. **282**, 3953 (2009)
17. G. Chen, C. Cheng, Chin. Phys. Lett. **25**, 3666 (2008)
18. A.N. Soldatov, Y.P. Polunina, Proc. SPIE **6938**, 69380N-1 (2007)